

This article may be downloaded for personal use only. Any other use requires prior permission of the author and AIP Publishing. This article appeared in Matthew Pelton, Stephen K. O’Leary, Franco Gaspari, Stefan Zukotynski; The optical absorption edge of diamond-like carbon: A quantum well model. Journal of Applied Physics 15 January 1998; 83 (2): 1029–1035. <https://doi.org/10.1063/1.366793> and may be found at <https://doi.org/10.1063/1.366793>.

Access to this work was provided by the University of Maryland, Baltimore County (UMBC) ScholarWorks@UMBC digital repository on the Maryland Shared Open Access (MD-SOAR) platform.

Please provide feedback

Please support the ScholarWorks@UMBC repository by emailing scholarworks-group@umbc.edu and telling us what having access to this work means to you and why it’s important to you. Thank you.

RESEARCH ARTICLE | JANUARY 15 1998

The optical absorption edge of diamond-like carbon: A quantum well model

Matthew Pelton; Stephen K. O'Leary; Franco Gaspari; Stefan Zukotynski



Journal of Applied Physics 83, 1029–1035 (1998)

<https://doi.org/10.1063/1.366793>



Export
Citation

CrossMark

Articles You May Be Interested In

Dielectric measurements on oxidized and hydrogenated chemical vapor deposited diamond films

Journal of Applied Physics (May 2002)

Ga Ohmic contact for *n*-type diamond by ion implantation

Appl. Phys. Lett. (March 2000)

Dominant defect levels in diamond thin films: A photocurrent and electron paramagnetic resonance study

Appl. Phys. Lett. (June 1998)

500 kHz or 8.5 GHz?
And all the ranges in between.

Lock-in Amplifiers for your periodic signal measurements



Find out more



The optical absorption edge of diamond-like carbon: A quantum well model

Matthew Pelton,^{a)} Stephen K. O'Leary,^{b)} Franco Gaspari, and Stefan Zukotynski
Department of Electrical and Computer Engineering, University of Toronto, Toronto, Ontario,
M5S 3G4, Canada

(Received 22 July 1996; accepted for publication 16 October 1997)

This article presents an analysis of the optical absorption edge of diamond-like carbon, based on transitions between confined electronic states in quantum wells. This theory is proposed to replace the commonly-used Tauc and Urbach expressions. It uses the cluster model of sample structure: the wells correspond to islands of graphitic, sp^2 -bonded material embedded in a diamond-like, sp^3 -bonded skeleton. A percolation model is used to give the cluster size distribution. Near-edge optical absorption coefficients are determined approximately for macroscopic thin films that have low fractions of sp^2 bonding. Experimental results provide preliminary confirmation of the approach. © 1998 American Institute of Physics. [S0021-8979(98)07202-8]

I. INTRODUCTION

The optical absorption edge of amorphous carbon has been the focus of considerable recent study. This absorption spectrum has been found to be unlike that of other amorphous semiconductors: the tail region is unusually broad; there are no clear regions of Tauc and Urbach behavior; and the apparent optical gap varies from practically zero to 5 eV, depending on the deposition parameters.¹ Although experimental spectra have been analyzed using the conventional Tauc and Urbach techniques, the parameters obtained have been inconsistent and have not had clear physical significance. It has been suggested that this problem is related to the unusual structural characteristics of the material, namely, the presence of both tetrahedral sp^3 bonding and trigonal sp^2 bonding.

The first explanation of the relation between bonding and optical absorption in amorphous carbon was provided by Robertson and O'Reilly.² They developed a two-phase structural model, in which sp^2 -bonded sites form compact clusters of sixfold, benzene-like rings within an sp^3 -bonded skeleton. This cluster model implies that the band gap fluctuates significantly in the material, changing rapidly at the cluster boundaries. The jumps in the band edges confine electrons within the graphitic islands, producing localized states.³ The localized energy levels depend on the sizes of the clusters: the more sixfold rings in the island, the lower the energies. This means that each cluster has an effective local energy gap that varies inversely with the cluster size. By averaging over these local gaps, Robertson obtained absorption edges that are qualitatively consistent with the observed edges.

Quantification of this model has been attempted. For example, Pascual and co-workers take the near-edge absorption coefficient in amorphous carbon to be a weighted sum of local absorption coefficients within graphitic clusters.⁴ They use Robertson's inverse relation between cluster size and local energy gap. However, they also assume parabolic densi-

ties of states (DOS) within the valence band (VB) and conduction band (CB) of the clusters; this is not an accurate representation of the deeply localized states that exist in the graphitic clusters. Finally, they assume that the distribution of cluster sizes is exponential; this assumption does not have a direct physical justification. An alternative formulation, by Dasgupta and co-workers, is based on the assumption of Gaussian DOS for π bonds throughout the material, to reflect the random distribution of cluster sizes.⁵ A similar treatment is given by Nesládek and co-workers.⁶ Although a normally distributed DOS seems intuitively reasonable, it has no strict physical justification. Finally, Mikulski and co-workers developed a formulation based on transitions between bonding and antibonding π states within the graphitic clusters, consistent with the Robertson model.⁷ However, they, too, use a cluster size distribution that is based more on convenience than on physical reality. All three models, in other words, begin with certain aspects of the Robertson model, but then introduce *ad hoc* assumptions. As well, they end up with disposable fitting parameters in the final results, so that comparison to experiment will not necessarily provide clear physical justification for their theories.

In this article, an attempt is made to improve on the previous models by considering only the physical implications of Robertson's cluster model, i.e., by working out the cluster model complete. This new formulation, which we call the quantum well (QW) model, provides a quantitative estimate for the near-edge optical absorption coefficient in diamond-like carbon (DLC). DLC is a form of amorphous carbon in which most of the bonds have the sp^3 rather than the sp^2 configuration. It is chosen for consideration because it is of greater technological interest than graphitic carbon, and because its structure can be conveniently modeled using percolation theory. The energy states in the clusters are determined within the framework of the effective-mass approximation, and the optical absorption edge is then determined by a first-principles calculation.

It should be mentioned that the cluster model has recently been called into question, most notably by Robertson himself.⁸ It has been suggested that the cluster model is valid only for samples with low disorder, while real DLC films are often prepared under conditions of high disorder. However, the cluster model still provides the simplest explanation for

^{a)}Present address: Department of Applied Physics, Stanford University, Stanford, California 94305-4090.

^{b)}Present address: Department of Electrical, Computer, and Systems Engineering, Rensselaer Polytechnic Institute, Troy, New York, 12180-3590.

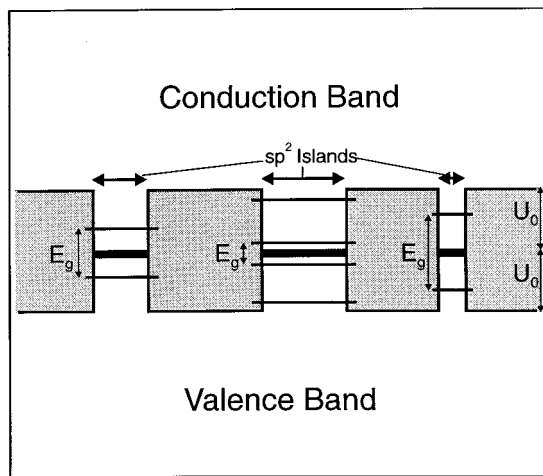


FIG. 1. Schematic band structure in the quantum-well model for diamond-like carbon. The band gap between the conduction band (CB) and the valence band (VB) varies between $2U_0$, in the sp^3 -bonded background, and zero, in the sp^2 -bonded islands. There is an abrupt transition in the position of band edges at the interfaces between the phases. This produces an effective potential jump U_0 for envelope wavefunctions in both bands, creating quantum wells. The confined energy levels in these wells are represented by horizontal lines; the energy difference between the ground states in the VB and CB wells is denoted E_g .

several observed phenomena, such as Raman spectra⁹ and luminescence characteristics.¹ As well, there have been reports of direct microscopic observation of graphitic clusters, consisting of sixfold rings, in amorphous carbon.¹⁰ If the predictions of the QW model are confirmed by experiment, this would provide additional support for the cluster model. It may, in fact, provide an experimental method to decide between it and competing structural models.

II. THE QUANTUM WELL MODEL

The QW formulation begins with a simplification of the cluster model. As in Robertson's original model, DLC is considered to consist of sp^2 -bonded islands embedded in an sp^3 -bonded skeleton. However, the amorphous character of the material is otherwise ignored: the diamond-like and graphitic phases are each treated as though they had the electronic characteristics of the corresponding crystalline material. In other words, the sp^3 background acts like diamond, a semiconductor with a wide band gap, while the sp^2 clusters act like graphite, a semiconductor with zero band gap (a semimetal).^{11,12} The transition between these two band gaps is assumed to occur abruptly at the boundaries of the graphitic clusters. If the band gap of diamond is denoted $2U_0$, the resulting band structure is as indicated in Fig. 1. The discontinuity in the band gap, occurring at the boundaries between sp^2 and sp^3 phases, is shared equally by the CB and the VB. Thus, each band edge jumps by U_0 at the limits of the sp^2 islands. This is related to the band model used in describing semiconductor heterostructures;¹³ a similar model has previously been used to describe the characteristics of hydrogenated amorphous silicon.¹⁴

In this analysis, carrier transport is described by the effective-mass approximation. Use of this phenomenological approach in the analysis of amorphous semiconductors is

well documented. The approximation should be quite accurate if the graphitic islands are large compared to the interatomic spacing.¹⁵ However, the effective-mass model has also been quite successful in describing much smaller structures, such as heterojunction quantum wells.¹⁶ Also, as will be explained below, large clusters, consisting of many atoms, primarily determine the characteristics of the absorption edge in the low-energy regime. Thus, the effective-mass treatment should be valid.

If the one-electron approximation is also used, a carrier in DLC can be described by an envelope wave function, which sees an effective potential defined by the band structure.¹⁷ This means that holes in the VB and electrons in the CB see a series of QWs, located at the positions of the graphitic clusters. The potential depth of the wells is U_0 , and the real-space sizes of the wells are equal to the sizes of the corresponding islands. A ladder of localized electronic states exists within the wells. Transitions between these confined states dominate optical absorption at energies significantly below U_0 .

The absorption spectrum near the fundamental edge, then, will depend on the energies of the localized states in the quantum wells. As in Robertson's analysis, the transition energy within a well will be inversely related to volume. The larger wells will contribute to optical absorption at lower energies, and vice versa. Through this relationship between well size and energy level, the shape of the spectrum will depend on the size distribution of the wells.

III. THE PERCOLATION MODEL

Determining exactly the cluster size distribution would be a prohibitively complex task. In order to make the problem manageable, the sixfold graphitic rings are assumed to be distributed throughout the sample in a random manner. In the limit where the number of such rings is small (i.e., in highly diamond-like samples), the effective interaction between rings will go to zero, and the approximation of no spatial correlation (statistical independence of location) should be good. In other words, the sp^2 -bonded rings are independently and uniformly distributed throughout the sample. The system can then be treated using a percolation model.

The sample is treated as though it were made up of an array of unit cells, each cell having a volume V_0 equal to the size of a single sixfold graphitic ring. For convenience, these cells are arranged in a simple cubic lattice (the effect of this choice is examined below). Each site in this lattice either contains a ring, and is said to be occupied, or it is part of the diamond-like background, and is said to be vacant. The rings are randomly distributed over the lattice, so that each site has an independent probability p of being occupied. If an sp^2 bond is taken to occupy the same volume as an sp^3 bond, and if the sample volume is large compared to V_0 (i.e., if the sample is macroscopic), then p is equal to the sp^2 bonding fraction (the fraction of all the bonds in the sample that have the sp^2 configuration).

In this percolation model, a graphitic island is represented by a cluster of adjacent occupied sites, two sites being defined as adjacent if they are nearest neighbors in the per-

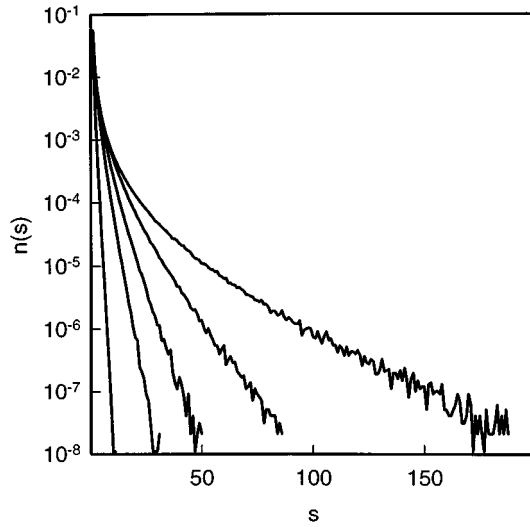


FIG. 2. Normalized cluster numbers $n(s)$ as a function of size s in the percolation lattice, as determined by numerical simulations. The curves, from left to right, correspond to $p=0.04$, $p=0.12$, $p=0.16$, $p=0.20$, and $p=0.24$, where p is the fraction of sites in the percolation lattice that are occupied.

colation lattice. The cluster number N_s is the number of clusters in the sample that consist of s occupied sites; it is divided by the total number of sites in the percolation lattice to give the normalized cluster number n_s . Above a critical probability $p=p_c$, known as the percolation threshold, there exists at least one cluster that extends across the entire lattice. For the simple cubic lattice used, numerical simulations give $p_c \approx 0.3117$.¹⁸ Above this threshold, the percolation model does not produce isolated sp^2 clusters, so that it can no longer be used to model the formation of quantum wells in DLC.

Approximate values of the normalized cluster numbers can be obtained by numerical simulations. In our calculations, periodic boundary conditions were used to reduce surface effects, and the results were averaged over 100 runs. Sample cluster numbers determined in a $100 \times 100 \times 100$ lattice are shown in Fig. 2. At large s , the results show scatter, due to the finite statistics used in the calculation. In a larger lattice, this noise is smaller; in the limit of a macroscopic sample, n_s varies smoothly with s . It is then reasonable to replace the sequence of cluster numbers with a continuous function $n(s)$.

Approximate analytical expressions for $n(s)$ can be developed. One of the most manageable of these is provided by Stauffer's scaling hypothesis.¹⁹ For $p < p_c$, in the limit of large s , this theory gives

$$n(s) \sim s^{-\tau} [C(p)]^s, \quad (1)$$

where C is a number that depends only on p , and τ is a critical coefficient. A field-theoretic argument gives $\tau=3/2$ in three dimensions.²⁰ Both the scaling expression, Eq. (1), and the value of τ are developed without reference to the cubic percolation lattice; only the value of $C(p)$ changes when a different lattice is used.

If the scaling assumption and the simulations agree, the numerical results should appear as straight lines on a plot of

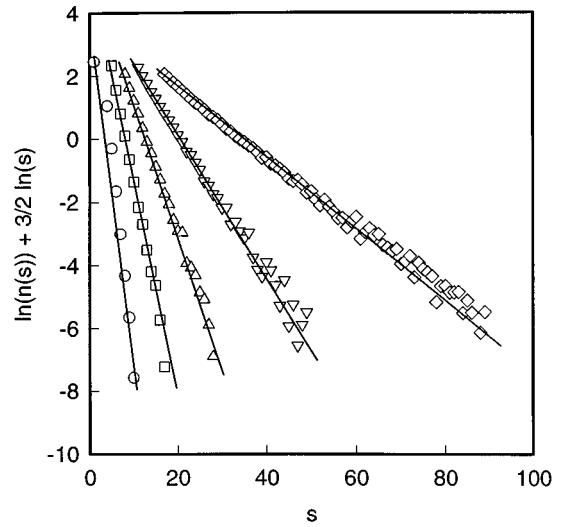


FIG. 3. Comparison of numerical results and the scaling formula for normalized cluster numbers $n(s)$ in the percolation lattice. The size of a cluster is s . The lines, from left to right, correspond to $p=0.04$, $p=0.08$, $p=0.12$, $p=0.16$, and $p=0.20$, where p is the fraction of sites in the percolation lattice that are occupied.

$\ln(n_s) + (3/2)\ln(s)$ vs s . This linearity was observed over a large range of s for several $p < p_c$, within the statistical scatter; see Fig. 3 for examples. The slopes of the lines give values of $C(p)$; sample results, as determined by a least-squares fitting algorithm, are reported in Table I. With these numbers and the scaling relation, it is possible to obtain the optical absorption spectrum.

IV. OPTICAL ABSORPTION

Determination of the optical absorption spectrum requires a consideration of transitions between initial states $|i\rangle$ and final states $|f\rangle$. Using the one-electron approximation,

TABLE I. Values of the constant $C(p)$ in the scaling expression for cluster number in the percolation model. The scaling formula is $n_s \sim s^{-3/2} [C(p)]^s$, where the normalized cluster number n_s is the number of clusters in the percolation lattice containing s sites, divided by the total number of sites, and p is the fraction of sites in the lattice that are occupied. Values of $C(p)$ were determined by fitting the scaling expression to cluster-number data determined by numerical calculations.

p	$C(p)$
0.02	0.119 ± 0.002
0.04	0.247 ± 0.004
0.06	0.368 ± 0.004
0.08	0.485 ± 0.006
0.10	0.574 ± 0.009
0.12	0.656 ± 0.009
0.14	0.743 ± 0.008
0.16	0.80 ± 0.01
0.18	0.86 ± 0.02
0.20	0.899 ± 0.007
0.22	0.95 ± 0.02
0.24	0.96 ± 0.01
0.26	0.98 ± 0.01

and assuming zero-temperature statistics, isotropy, and linear response, the absorption coefficient at frequency ω in a thin, weakly-absorbing film will be²¹

$$\alpha(\omega) = \frac{8\pi^2 e^2}{(m^*)^2 c \eta \omega V} \sum_{i,f} |\langle f|p|i\rangle|^2 \delta(E_f - E_i - \hbar\omega), \quad (2)$$

where m^* is the effective electron mass, η is the index of refraction, V is the total sample volume, p is the momentum operator, E_i is the energy of the initial state, and E_f is the energy of the final state.

As a first-order approximation, only transitions between the ground states of the VB and CB wells are considered. Transitions between other states involve higher energies, and thus do not make a significant contribution to the absorption coefficient near the edge. (As is discussed below, this was verified by direct calculations.) Transitions between bound states in different clusters will have lower momentum matrix elements $\langle f|p|i\rangle$ than transitions involving states within the same clusters; i.e., the spatial correlation of the VB and CB wells make spatially indirect transitions relatively unlikely. This means that we can adopt an approach similar to Jackson,²² and replace the momentum matrix elements with an average value \mathcal{P} . It also means that the sum in Eq. (2) reduces to a sum over the clusters.

The normalized cluster number is $n_s = N_s(V_0/V)$ where N_s is the number of clusters that consist of s sixfold rings, and V_0 is the volume of a single ring. Using this, Eq. (2) becomes

$$\alpha(\omega) = \frac{K}{\hbar\omega} \sum_s n_s \delta(E_g(s) - \hbar\omega), \quad (3)$$

where

$$K \equiv \frac{8\pi^2 \hbar e^2 |\mathcal{A}|^2}{(m^*)^2 c \eta V_0}. \quad (4)$$

Next, the cluster size distribution n_s is replaced with a continuous function $n(s)$, and the sum over s is converted into an integral. The function $E_g(s)$ can then be inverted to give $s(E_g)$, the size of well needed to support an energy gap of magnitude E_g . Since this function will be monotonically decreasing, integration gives

$$\alpha(\omega) = \frac{K}{\hbar\omega} \left[\left| \frac{ds}{dE_g} \right| n(s) \right]_{E_g = \hbar\omega}. \quad (5)$$

In this equation, s is a function of E_g , and the terms in the square brackets are evaluated at $E_g = \hbar\omega$. Since an expression for $n(s)$ has already been given in Eq. (1), all that remains to be determined is the function $s(E_g)$.

For simplicity, the clusters are taken to be spherically symmetric. As well, they are assumed to be sufficiently distant from one another that bound-state wave functions from adjacent QWs do not overlap. The energies E of the ground states are then given by the lowest-valued solutions of the following equation:²³

$$\tan\left(\frac{\sqrt{2m^*(U_0 - |E|)}}{\hbar} L\right) = -\sqrt{\frac{U_0 - |E|}{|E|}}, \quad (6)$$

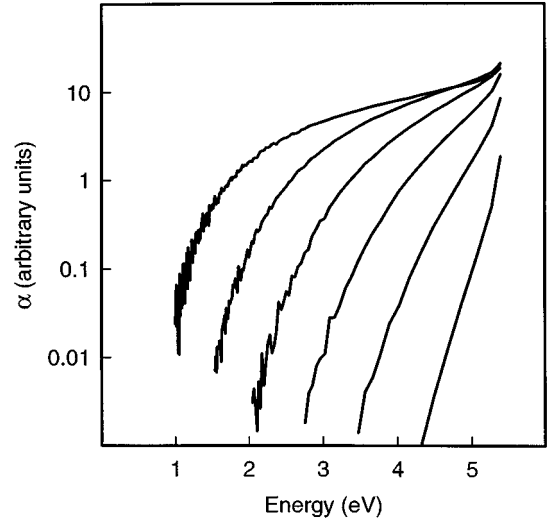


FIG. 4. Numerically calculated absorption edges in DLC. The absorption coefficient α is shown as a function of photon energy. The curves, from left to right, correspond to $p=0.04$, $p=0.08$, $p=0.12$, $p=0.16$, $p=0.20$, and $p=0.24$, where p is the sp^2 bonding fraction.

where L is the radius of the well.

The next assumption is that the VB and CB wells are described by the same depth U_0 and the same effective mass m^* . This gives

$$E_g = 2(U_0 - |E|). \quad (7)$$

This equation can be combined with Eq. (6) to give the following first-order expression, in the limit $E_g \ll U_0$:

$$s(E_g) \approx \frac{A}{V_0} \left(\frac{\pi^3}{x^{3/2}} \right), \quad (8)$$

where $A \equiv (4\pi/3)(\hbar^2/2m^*U_0)^{3/2}$ and $x \equiv E_g/2U_0$. The derivation of this expression is outlined in the Appendix.

V. RESULTS

The absorption coefficient can be evaluated numerically using Eq. (3). The function $E_g(s)$ in this expression must be converted into a function of the cluster radius L :

$$E_g(s) \leftrightarrow E_g \left[L = \left(\frac{3}{4\pi} V_0 s \right)^{1/3} \right]. \quad (9)$$

This function, in turn, is given by Eqs. (6) and (7); the former equation can be solved numerically for the ground-state energy $|E|$. The normalized cluster numbers n_s come from the numerical calculations described in Sec. III. Determination of α is then a matter of numerical substitution.

Absorption coefficients calculated using this method, for several values of p below p_c , are shown in Fig. 4. In these calculations, the following parameters were used. The volume of a single sixfold ring is $V_0 \approx 8.8 \text{ \AA}^3$.²⁴ The refractive index η is taken to be that of graphite, approximately 2.²⁵ The well depth U_0 is assumed to be 2.7 eV, half the energy gap of diamond at absolute zero temperature.²⁶ The momentum matrix element $|\mathcal{A}|$ is of the order \hbar/L_0 , where L_0 is the

radius of a single sixfold ring. The effective mass m^* is taken to be equal to the free electron mass (this assumption is discussed below).

In addition to these numerical results, an analytical formula can also be derived. Combining Eqs. (1), (5), and (8):

$$\alpha(\omega) \sim x_0^{-5/4} [C(p)]^{(A\pi^3/V_0)x_0^{-3/2}}, \quad (10)$$

where

$$x_0 \equiv \frac{\hbar\omega}{2U_0}. \quad (11)$$

This expression represents the final result for the optical absorption edge of DLC in the QW model.

VI. DISCUSSION

The predictions of the QW model are insensitive to most of the assumptions made. Specifically, direct calculation of the absorption edges showed that they are not affected significantly if the well depth U_0 is different from that assumed, if the effective mass m^* is not the same in the sp^3 and sp^2 phases, if the VB and CB wells are not identical, if the graphitic clusters exhibit a small band gap, or if temperature effects are considered. Similar calculations also showed that the absorption coefficient depends strongly on the volume of a single sixfold ring; however, since this value is well known, its sensitivity is not important.

More significant is the fact that the predictions of the QW model are sensitive to changes in the effective mass. Since an accurate value of effective mass in the graphitic clusters is essentially impossible to obtain, it is perhaps best to treat m^* as an adjustable parameter. It will then incorporate the effects of all the assumptions made in formulating the QW model and in choosing the other parameters, and can also be thought of as an effective average of the CB and VB masses. The best fit to experimental data may therefore be obtained by using a value for m^* that differs from the actual conduction effective mass.

Another important factor is the choice of a simple cubic lattice for the percolation model. This particular choice of structure is arbitrary: it does not correspond to any physical property of the system. A different percolation lattice could just as well be used; however, this would have no serious effect on the results. The scaling equation, Eq. (1), is determined without reference to the form of the percolation lattice; likewise, the value of the critical coefficient τ is the same for any three-dimensional structure. All that changes when a different lattice is used is the value of the parameter $C(p)$. However, this constant is also the only way that the sp^2 bonding fraction p affects the absorption spectrum. Using a different percolation lattice structure would thus be equivalent to using a different set of values for p . This means that comparison of absorption data to Eq. (10) is not a good way to determine film composition. Rather, absorption data should be compared to the equation only for films whose composition has been independently determined.

When experimental data is compared to the QW model, it is important to remember that the model does not predict the absorption coefficient exactly over all energies for all

samples. For example, since the coupling of bound-state wavefunctions between adjacent QWs is assumed to be negligible, only samples with a low graphitic content can be considered. This limit is also required by the use of the sub-threshold percolation model, and by the assumption that the locations of the sixfold rings in the sample are random. The requirement that $p < p_c$, for example, means that the only films that can be treated using the QW model are those with less than about 30% sp^2 bonding. Another restriction comes from the fact that the only optical transitions considered are between ground states in individual clusters. When the energy of incident light is comparable to the band gap of the diamond-like phase, other types of transitions become important. As well, the cluster number scaling equation and the effective-mass approximation are most accurate for large islands; in fact, the effective-mass model should not be used when the cluster size is comparable to the interatomic spacing. Since the largest clusters have the lowest-lying ground states, they correspond to the lowest-energy transitions. The QW model thus applies only in the low-energy limit $E_g \ll U_0$. This limit is also required by the use of the Taylor-series expansion, Eq. (8). In other words, applicability of the model is restricted to the near-edge limit $\alpha \rightarrow 0$.

The accuracy of the model in this limit was tested by modifying the calculations to include a consideration of transitions between deeper-lying states in the QWs. This directly verified that these higher-order transitions do not make a significant contribution to the form of the optical absorption edge in the low-energy limit. It was also directly verified that the scaling equation becomes highly accurate in the limit of large cluster number (see Fig. 3). The QW model, in other words, should provide a good representation of the low-absorption tail of the fundamental edge in highly diamond-like films.

Of course, this is only true if the cluster model, the basis of the analysis, is correct. If the predictions of the QW model are consistent with experiment, though, this would provide support for the cluster model. Since the structure of DLC is currently the subject of discussion, such evidence for a particular model would be of some importance.

VII. COMPARISON TO EXPERIMENT

The optical absorption edges of amorphous semiconductors are most often analyzed using two formulas. The first is the Tauc expression:

$$\omega\alpha \sim (\hbar\omega - E_T)^2, \quad (12)$$

where E_T is known as the Tauc optical gap. The second, due to Urbach, is

$$\alpha \sim \exp\left(\frac{\hbar\omega - \hbar\omega_0}{E_0}\right), \quad (13)$$

where $\hbar\omega_0$ is called the Urbach focus or Urbach parameter, and E_0 is an adjustable parameter that represents the width of the absorption edge. The QW-model formula for the optical absorption edge, Eq. (10), is not similar to either of these expressions. This is not unexpected: the assumptions involved in deriving the Tauc and Urbach equations are not

valid in the case of DLC. The Tauc formula applies for transitions between a continuous VB and CB, each with a parabolic DOS.²⁷ In DLC, though, near-edge transitions are between localized states in the sp^2 clusters, not between continuous bands. The Urbach expression, on the other hand, can be obtained by assuming that electrons move in a Gaussian-correlated random potential profile.²⁸ Such a potential does not exist in DLC, where large fluctuations in the band gap occur at the positions of graphitic clusters, which are not normally distributed. The characteristics of DLC, in other words, are such that the Tauc and Urbach models are not likely to be valid.

This is consistent with the experimental results reported in the literature. There has been little agreement among the parameters obtained by application of Tauc and Urbach analyses to DLC. This, we believe, is not due to difficulties with the experimental data; rather, the problem is that the standard models do not apply. If a Tauc or Urbach fit is attempted, the slope and intercept of the line obtained will depend on the range of absorption coefficient considered. This means that the fitted value of E_T or E_0 will have no direct physical meaning.

To determine whether the QW analysis is more physical, its predictions must be compared to experiment. When performing such a comparison, it is important to remember that the sp^2 bonding fractions of the films to be analyzed should be obtained by a separate method, and that the effective mass m^* serves more as an adjustable fitting parameter rather than as a physical mass. Apart from this mass, there are no free parameters: all other variables are either independently measured properties of the material, or are inherent in the QW model.

A comparison to experiment was performed by measuring optical absorption on a DLC sample, 0.1 μm thick, deposited on a quartz substrate using the saddle-field glow-discharge method.²⁹ Similar films have been previously characterized by x-ray photoelectron spectroscopy (XPS), x-ray stimulated Auger electron spectroscopy (XAES), and Raman spectroscopy, and the sp^2 content has been determined to be approximately 25 at %.³⁰ The transmittance and the reflectance of this film were measured using a Perkin Elmer Lambda 18 UV/Visible spectrophotometer; the absorption coefficient was then calculated following Demichelis *et al.*³¹ These experimental data were compared to the final formula for the optical absorption coefficient in the QW model, Eq. (10). Using an effective mass of 0.94 times the free electron mass and an sp^2 fraction of 0.27, the fit shown in Fig. 5 was obtained. The effective mass used is reasonable for an amorphous semiconductor, and the value of p is quite close to the experimental value.

However, these measurements involve relatively high values of absorption coefficient; a better comparison would involve lower values, where the QW model is expected to be more accurate. Reflectance/transmittance methods cannot measure such low values; alternative methods such as photothermal deflection spectroscopy (PDS) are necessary. Compagnini and co-workers have performed such measurements,³² their results were also compared to Eq. (10), as shown in Fig. 5. The same effective mass was used

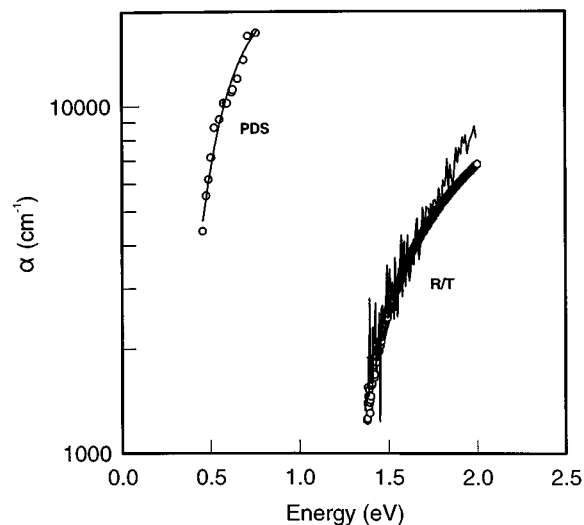


FIG. 5. Comparison of experimental data to QW model predictions. The absorption coefficient α is shown as a function of photon energy. The open symbols are data from our reflectance/transmittance measurements (R/T), and photothermal deflection spectroscopy data from Ref. 32 (PDS); the solid lines are fits using Eq. (10).

as in the previous comparison, while p was taken to be 0.21. This value compares well with the sp^2 bonding fraction of 0.24 that Compagnini *et al.* determined by energy electron loss spectroscopy (EELS).

Even these data, though, involve absorption coefficients greater than the range in which the QW model is expected to be most accurate. Unfortunately, to our knowledge, there exist no reliable measurements of very low absorption in DLC films with very high sp^3 fractions. Such measurements would be necessary to provide a critical test of the QW model. This, in turn, would help decide between the currently competing structural models for the material. Despite their limitations, though, the available comparisons to experimental results can be considered a preliminary confirmation of the QW model.

VIII. CONCLUSIONS

A quantum well description of the optical absorption edge in DLC thin films has been developed, based on the cluster model of the material structure. The analysis considers transitions between localized electronic states within graphitic clusters. The theory is developed for low values of the absorption coefficient (i.e., the near-edge region) and low values of the sp^2 bonding fraction (i.e., highly diamond-like films). Although a number of assumptions are involved in formulating the model, none of them are *ad hoc*. In other words, the QW model should be valid as long as the cluster model is valid. If the QW model is able to predict the characteristics of optical absorption edges in DLC, this will provide support for the cluster model.

The final formula for the optical absorption edge is given by Eq. (10). The quantitative results will depend on the choice of modeling parameters; however, the form of the equation is universally valid within the regime of applicability. The effective mass m^* serves as an adjustable modeling

parameter for comparison to experimental results. Good preliminary agreement between experiment and model predictions was obtained.

ACKNOWLEDGMENTS

Financial assistance from the Natural Sciences and Engineering Research Council of Canada is gratefully acknowledged. One of the authors (M. P.) gratefully acknowledges support through a Canada Scholarship. Another (S. K. O.) gratefully acknowledges a Natural Sciences and Engineering Research Council of Canada Postdoctoral Fellowship. Thanks are also due to Professor R. C. Desai for interesting discussions.

APPENDIX

The derivation of a formula for $s(E_g)$ begins with Eq. (6). This expression can be rearranged to give the well volume as a function of energy:

$$V_w(E) = \frac{4}{3} \pi L^3 = \frac{A}{(1 - |E|/U_0)^{3/2}} \times \left(\pi - \arctan \sqrt{\frac{1 - |E|/U_0}{|E|/U_0}} \right)^3, \quad (14)$$

where

$$A \equiv \frac{4\pi}{3} \left(\frac{\hbar^2}{2m^*U_0} \right)^{3/2}. \quad (15)$$

A cluster of size V_w will consist of s six-fold rings, each with size V_0 , such that $V_w = sV_0$. Using this and Eq. (7), Eq. (14) becomes

$$s(E_g) = \frac{A}{V_0 x^{3/2}} \left(\pi - \arctan \sqrt{\frac{x}{1-x}} \right)^3, \quad (16)$$

where

$$x \equiv E_g/2U_0. \quad (17)$$

For $E_g \ll U_0$, this expression can be expanded as a series in x . Retaining only the first term, Eq. (8) is obtained.

¹D. Dasgupta, C. De Martino, F. Demichelis, and A. Tagliaferro, J. Non-Cryst. Solids **164–166**, 1147 (1993).

²J. Robertson and E. P. O'Reilly, Phys. Rev. B **35**, 2946 (1987).

³J. Robertson, Philos. Mag. B **66**, 199 (1992).

- ⁴E. Pascual, C. Serra, and E. Bertran, J. Appl. Phys. **70**, 5119 (1991).
⁵D. Dasgupta, F. Demichelis, C. F. Pirri, and A. Tagliaferro, Phys. Rev. B **43**, 2131 (1991).
⁶M. Nesládek, K. Meykens, L. M. Stals, M. Vaněček, and J. Rosa, Phys. Rev. B **54**, 5552 (1996).
⁷P. Mikulski, J. Patyk, and F. Rozploch, J. Non-Cryst. Solids **176**, 230 (1994).
⁸J. Robertson, Diamond Relat. Mater. **4**, 297 (1995).
⁹R. E. Schroder, R. J. Nemanich, and J. T. Glass, Phys. Rev. B **41**, 3738 (1990).
¹⁰B. Marchon, M. Salmeron, and W. Siekhaus, Phys. Rev. B **39**, 12 907 (1989).
¹¹P. R. Wallace, Phys. Rev. **71**, 622 (1947).
¹²N. A. W. Holzwarth, S. G. Louie, and S. Rabii, Phys. Rev. B **26**, 5382 (1982).
¹³C. Weisbuch and B. Vinter, *Quantum Semiconductor Devices* (Academic, San Diego, 1991).
¹⁴S. K. O'Leary, S. Zukotynski, and J. M. Perz, J. Appl. Phys. **72**, 2272 (1992).
¹⁵H. Haug and S. W. Koch, *Quantum Theory of the Optical and Electronic Properties of Semiconductors* (World Scientific, Singapore, 1990).
¹⁶M. Altarelli, in *Heterojunctions and Semiconductor Superlattices*, edited by G. Allen, G. Bastard, N. Boccara, M. Lannoo, and M. Voos (Springer, New York, 1985), p. 12.
¹⁷S. K. O'Leary, S. Zukotynski, and J. M. Perz, J. Appl. Phys. **78**, 4282 (1995).
¹⁸D. Stauffer, *Introduction to Percolation Theory* (Taylor & Francis, London, 1985).
¹⁹H. Nakanishi and H. E. Stanley, Phys. Rev. B **22**, 2466 (1980).
²⁰G. Parisi and N. Sourlas, Phys. Rev. Lett. **46**, 871 (1981).
²¹P. Voisin, in *Heterojunctions and Semiconductor Superlattices*, edited by G. Allen, G. Bastard, N. Boccara, M. Lannoo, and M. Voos (Springer, New York, 1985), p. 73.
²²W. B. Jackson, S. M. Keslo, C. C. Tsai, J. W. Allen, and S.-J. Oh, Phys. Rev. B **31**, 5187 (1985).
²³C. Cohen-Tannoudji, in *Quantum Mechanics* (Wiley, Toronto, 1977), Vol. I.
²⁴J. Robertson, Surf. Coat. Technol. **50**, 185 (1992).
²⁵B. T. Kelly, *Physics of Graphite* (Applied Science Publishers, London, 1981).
²⁶C. Kittel, *Introduction to Solid State Physics*, 7th ed. (Wiley, Toronto, 1996).
²⁷J. Tauc, in *Amorphous and Liquid Semiconductors*, edited by J. Tauc (Plenum, New York, 1974), p. 159.
²⁸S. John, C. Soukoulis, M. H. Cohen, and E. N. Economou, Phys. Rev. Lett. **57**, 1777 (1986).
²⁹R. V. Kruzelecky and S. Zukotynski, in *Plasma Properties, Deposition, and Etching: Materials Science Forum*, Vol. 140–142, edited by J. J. Pouch and S. Alterovitz (Trans Tech Publications, Ltd., Aedermannsdorf, Switzerland, 1993), p. 89.
³⁰P. K. Lim, F. Gaspari, and S. Zukotynski, J. Appl. Phys. **78**, 5307 (1995).
³¹F. Demichelis, G. Kaniadakis, A. Tagliaferro, and E. Tresso, Appl. Opt. **26**, 1737 (1987).
³²G. Compagnini, U. Zammit, K. N. Madhusoodanan, and G. Foti, Phys. Rev. B **51**, 11168 (1995).